



Ni/HZSM-5 catalysts for hydrodeoxygenation of polycarbonate plastic wastes into cycloalkanes for sustainable aviation fuels

Jieyi Liu^a, Junde Wei^a, Xiao Feng^d, Mingxia Song^a, Song Shi^d, Sibao Liu^{a,b,*}, Guozhu Liu^{a,b,c,*}

^a Key Laboratory for Green Chemical Technology of Ministry of Education, School of Chemical Engineering and Technology, Tianjin 300072, China

^b Haihe Lab of Sustainable Chemical Transformations, Tianjin 300192, China

^c Zhejiang Institute of Tianjin University, Ningbo, Zhejiang 315201, China

^d State Key Laboratory of Catalysis, Dalian Institute of Chemical Physics, Chinese Academy of Sciences, Dalian 116023, China

ARTICLE INFO

Keywords:

Polycarbonate plastic wastes

Hydrodeoxygenation

HZSM-5

Nickel

Sustainable aviation fuel

ABSTRACT

Hydrodeoxygenation (HDO) is one of the effective methods for upcycling polycarbonate (PC) plastic waste, but the development of low-cost, high-performance HDO catalysts still faces great challenges. In this work, we report that a bifunctional Ni/HZSM-5 catalyst can directly upgrade PC plastic wastes into sustainable aviation fuel ranged cycloalkanes in high yields (99.3 %) with 81.2 % yield of C₁₅ dicycloalkane under mild reaction conditions (190 °C, 4 MPa H₂). Controlled reactions of PC and probe molecules demonstrated the conversion of PC into C₁₅ dicycloalkanes involves PC depolymerization by direct cleavage of C-O bonds adjacent to benzene ring and ester group, forming C₁₅ aromatics and C₁₅ monophenols at the metal sites, followed by hydrogenation of C₁₅ aromatics rings on metallic Ni sites and HDO of C₁₅ monophenols on metal-acid dual sites parallel to generate C₁₅ dicycloalkane. The C-C cracking mainly occurred on the tertiary carbon adjacent to the benzene ring on acidic sites of HZSM-5, thus forming C₆~C₉ monocyclic alkanes. The realization of this process can be attributed to the cooperation between metal sites and acid centers on Ni/HZSM-5. Besides, the metal-acid balance (MAB) in Ni/HZSM-5 significantly affected the HDO activity and product distribution. 20Ni/HZSM-5(200) with suitable MAB showed good HDO activity and excellent selectivity to C₁₅ dicycloalkane. In addition, the obtained catalyst was also capable of converting common real PC plastics wastes (CD disk, DVD disk and PC sheet) into cycloalkanes with the yield up to 98 % and exhibited excellent stability. This approach to construct inexpensive bifunctional catalysts highlights an efficient and reliable route for HDO of PC to sustainable aviation fuel, providing a new avenue towards a circular economy.

1. Introduction

Chemical upcycling of plastic wastes is an essential part of the circular economy and addresses global environmental problems and energy loss issues [1–5]. Polycarbonate (PC) is a principal engineering plastic, which has been widely used in packaging, transportation, construction and electronic industry, due to its transparency, thermal stability, excellent toughness, and a very good dimensional stability [6]. PC has an annual production of ~6 million tons and the global demand now is rising [7]. As a result, there is a rising need for recycling. Unfortunately, due to lack of efficient technology, only a limited quantity of this material is recycled (~9 %) [8–11].

For the PC upcycling into value-added products, different chemical

methods have been reported including pyrolysis, hydrolysis, alcoholysis, glycolysis and aminolysis [12–18]. Pyrolysis is an energy-consuming process, which needs high reaction temperature. In addition, the product selectivity is very hard to control [19,20]. Trans-esterification is an efficient way to obtain the monomers from PC. However, the principal limitation of such process is the need of excessive solvent and corrosive homogeneous catalysts and the formation of difficult separated side products [9,18]. Consequently, developing new chemical process for valorization of PC plastic wastes into new products will be transformative.

Sustainable Aviation Fuels (SAF) are defined as renewable or waste-derived aviation fuels that meets sustainability criteria [21–25]. Using SAF results in a reduction in carbon emissions compared to the

* Corresponding authors at: Key Laboratory for Green Chemical Technology of Ministry of Education, School of Chemical Engineering and Technology, Tianjin 300072, China.

E-mail addresses: liusibao@tju.edu.cn (S. Liu), gliu@tju.edu.cn (G. Liu).

<https://doi.org/10.1016/j.apcatb.2023.123050>

Received 4 April 2023; Received in revised form 5 June 2023; Accepted 26 June 2023

Available online 1 July 2023

0926-3373/© 2023 Elsevier B.V. All rights reserved.

traditional jet fuel. Cycloalkanes are the major components of aviation fuels. Hydrodeoxygenation (HDO) of PC plastic can yield propane-2, 2-diylidicyclohexane, which has excellent properties (e.g., high density and high volumetric heat values) for SAF [8,26]. With this, the HDO of PC wastes will provide a new pathway for the production of sustainable aviation fuel (SAF). However, there has been limited research.

Recently, Li et al. firstly reported the production of aviation fuel ranged polycycloalkanes through a two-step route including the methanolysis of PC waste to bisphenol A and followed HDO over Pt/C + H β catalytic system [27]. The yield of C₁₃~C₁₅ polycycloalkanes could reach to ~80 %. To simplify the process, the same group demonstrated a one-step aqueous phase HDO process for the direct conversion of PC to polycycloalkanes. A very high yield (94.9 %) of target propane-2, 2-diylidicyclohexane can be obtained by using Rh/C + USY catalytic system at 200 °C, 3.5 MPa H₂ for 12 h [28]. However, noble metal catalysts are used, which is not beneficial for practical applications. To lower the expense, Raney Ni + USY catalyst was adopted for one-pot transfer HDO of PC by using isopropanol as both solvent and hydrogen donor [29]. However, only ~30 % yield of C₆~C₁₅ cycloalkanes can be achieved at 250 °C. Therefore, it is desirable to develop inexpensive HDO catalysts for the conversion of PC plastic wastes to cycloalkanes in high yield under mild reaction conditions.

The process for HDO of PC to cycloalkanes is very complex, including the hydrogenation of the benzene ring, the cleavage of C-O bonds, and even C-C cracking [8,30,31]. The C-C bonds are easily cleaved at the quarter carbon position during HDO process, which makes the production of propane-2,2-diylidicyclohexane difficult [32,33]. Therefore, a key challenge of attaining high yield cycloalkanes, especially propane-2, 2-diylidicyclohexane, is to identify a catalyst that enables the selective cleavage of C-O bonds while preserving C-C bonds. Bifunctional metal-acid catalysts (e.g., Ni/HZSM-5) have been reported to effectively catalyze the HDO of biomass, including bio-oils [34,35], lignin [36], phenols [37–40], fatty acids [41], vegetable oils [41] and furans [42, 43], into hydrocarbons in high yield. Inspired by this, we think that these catalysts are potential for the HDO of PC to cycloalkanes. So far, no such catalyst has been developed.

Herein, we report a bifunctional Ni/HZSM-5 catalyst that can direct HDO of PC plastic wastes into aviation fuel range cycloalkanes in high yields (99.3 %) under mild conditions (190 °C, 4 MPa H₂). The yield of propane-2,2-diylidicyclohexane (hereinafter referred to as C₁₅ dicycloalkane) could reach to 81.2 %. The catalyst is also active for conversion of different PC plastic wastes including chopped DVD disk, CD disk and PC sheet. Controlled reactions of PC and probe molecules as well as catalyst characterization were conducted to elucidate the reaction pathway for PC conversion and the cooperative functions of metal-acid dual sites in Ni/HZSM-5. In addition, the catalyst can be reused at least 6 times without loss in activity. The application of non-noble Ni/HZSM-5 catalyst could effectively reduce the cost of chemical upcycling of PC plastic wastes to valuable aviation fuel ranged cycloalkanes, which will open a new avenue for a circular economy.

2. Experimental

2.1. Chemicals and materials

Ni(NO₃)₂·6 H₂O (98 wt %), cyclopentane (C₅H₁₀, ≥96.0 %), and *n*-tetradecane (C₁₄H₃₀, ≥98.0 %) were supplied by Aladdin Chemical Reagent Co., Ltd. The HZSM-5 zeolites (SiO₂/Al₂O₃ = 25, 60, 130, 200, 360) were purchased from Nankai University Catalyst Co. Ltd.

In this study, pure poly(bisphenol A carbonate) (PC) pellets (product number: P888352, average molecular weight: 26000, 2 mm length × 2 mm diameter from Shanghai Macklin Biochemical Technology Co., Ltd.) were used to simulate the PC waste. To check the catalyst application for conversion of real plastic wastes, we also used DVD disk, CD disk and PC sheet (the representatives of real PC) as the substrate for activity test. Before the activity test, the DVD disk and CD disk was polished with a

sandpaper to remove the metal layer, washed thoroughly with ethanol, and cut into 2 mm × 2 mm pieces with scissors.

2.2. Catalysts preparation

Ni/HZSM-5 catalyst was prepared using the impregnation method. Typically, firstly, HZSM-5 were pretreated by calcination in a muffle furnace at 550 °C for 4 h with a ramping rate of 2 °C/min. Then HZSM-5 was impregnated with a certain amount of Ni(NO₃)₂ aqueous solution. After evaporation at 67 °C on a hot plate and drying at 80 °C for 12 h, Ni/HZSM-5 was obtained. Ni/HZSM-5 was reduced with 30 mL/min H₂ flow at 500 °C for 2 h with a heating rate of 10 °C/min and cooled down with N₂ flow to room temperature. Then the catalyst was passivated with 2 % O₂/N₂ and was ready for use. HZSM-5 with different SiO₂/Al₂O₃ (molar ratio = 25, 60, 130, 200, 360) were chosen as supports. The nickel loading ranged from 2.5 wt % to 30 wt %. The catalyst was labeled as xNi/HZSM-5(y), wherein x and y stand for the Ni loading amount and SiO₂/Al₂O₃ ratio, respectively.

For comparison, the Silicalite-1 zeolite was also employed for the preparation of 20Ni/S-1 catalyst with the same procedure as that for Ni/HZSM-5 catalyst. The nickel loading of the 20Ni/S-1 catalyst was 20 wt %. Silicalite-1 zeolite was synthesized under hydrothermal condition at 170 °C for 96 h. The molar composition of mixing gel was 1.0 SiO₂: 35 H₂O: 0.4 TPAOH. Typically, 15 g deionized water was mixed with 13 g TPAOH solution and then add 8.32 g TEOs dropwise. The mixing gel was stirred continuously for 6 h until the solution clear and then transferred the gel in a 100 mL Teflon-lined stainless steel autoclave. The crystallization process was carried out in an oven at 170 °C for 96 h. The obtained solid was washed with ethanol and water for several times. The products were dried at 80 °C for 12 h, followed by calcination at 550 °C for 6 h.

2.3. Activity tests

The HDO of PC was carried out in a 50 mL Parr reactor with an inserted glass liner under hydrogen atmosphere. For each test, 0.3 g PC, 15 mL cyclopentane, 0.1 g catalyst were charged into the glass liner. Then, the reactor was pressurized with N₂ (1 MPa) three times to purge out the air. After that, the reactor was filled to 4 MPa with H₂. The HDO test was carried out at 190 °C and 500 rpm. After a certain reaction time, the reactor quenched to room temperature in an ice-water bath. Upon cooling, the pressure was released. The liquid product along with spent catalyst was collected by using additional 10 mL cyclopentane with *n*-tetradecane as an internal standard. The structures of products were identified by using GC-MS (Shimadzu GCMS-QP2020) with a Rtx-5MS capillary column. The liquid products were quantitatively analyzed by GC (Agilent 7890 A) equipped with an HP-PONA column and a flame ionization detector. The gaseous products from the HDO of PC were analyzed by GC (Shimadzu 2014) equipped with a TCD detector and an FID detector using a packed column (carbon molecular sieve TDX-01) and PLOT Q capillary column, respectively.

The yields of products were calculated according to following equation:

Yield of detected products (%)

$$= \frac{\text{mol product} \times \text{C atoms in product}}{\text{mol of total C atoms of initial aromatic reactant}} \times 100$$

In the catalyst recyclability tests, the used catalyst after each cycle was collected by centrifugation. Then the obtained spent catalysts were washed three times with 10 mL of cyclopentane, dried at 80 °C for 12 h, and then calcined at 500 °C for 3 h at a heating rate of 10 °C/min. Before the activity test, the catalyst was reduced and passivated again.

2.4. Catalysts characterizations

X-ray diffraction (XRD, D8 Focus, Bruker) was used to determine the structural properties of the catalysts on a X-ray diffraction with (Cu K α , $\lambda = 1.541 \text{ \AA}$) radiation at 40 kV and 40 mA in the 2θ range from 10° to 80° at a speed of $8^\circ/\text{min}$. The morphology and structure of the catalysts were determined by scanning electron microscopy (SEM, Apreo S, FEI) and transmission electron microscopy (TEM, JEM-2100 F, JEOL).

The nitrogen adsorption/desorption isotherms were obtained by using an ASAP 2460 analyzer (Micromeritics, USA). Prior to test, the catalyst was degassed at 300°C for 6 h. The BET surface area of the samples was determined by Brunauer-Emmett-Teller (BET) equation. The micropore volume (V_{micro}) and mesopore volume (V_{meso}) were analyzed by using t-plot and Barrett-Joyner-Halenda (BJH) methods, respectively.

Ni dispersions were measured by hydrogen chemisorption using dynamic pulse method. Catalyst samples (0.1 g) were reduced in-situ at 500°C for 2 h ($10^\circ\text{C}/\text{min}$) in 30 mL/min H_2 flow. Then pre-reduced samples were cooled to 50°C in Ar flow (30 mL/min). Pure H_2 doses were delivered until complete saturation. Ar was passed through the reactor to remove the weakly adsorbed H_2 from the catalyst.

Ammonia temperature-programmed desorption (NH_3 -TPD) was carried out with a Chemisorption Physorption Analyzer (DAS-7200, Huasi) equipped with a thermal conductivity detector (TCD). For each NH_3 -TPD test, the catalysts were reduced in H_2 at 500°C for 2 h with a heating rate of $10^\circ\text{C}/\text{min}$. After being cooled to 100°C in He flow (30 mL/min), NH_3 adsorption was performed by a mixture of NH_3 and He (10 % NH_3 in He) at 100°C for 60 min. After removing the weakly adsorbed NH_3 from the catalyst in He flow for 2 h, the desorbed NH_3 was monitored in the range of $100\text{--}600^\circ\text{C}$ with a ramping rate of $10^\circ\text{C}/\text{min}$.

Determination of acid type and concentration was carried out on a Bruker Tensor 27 IR spectrometer by pyridine adsorption. Press the catalyst into a sample disc with a diameter of about 12.2 mm with a mold, then the sample disc was placed into the infrared cell connected to a closed glass vacuum system. The sample was firstly pretreated at 400°C for 60 min in vacuum to remove adsorbed species. Then it was cooled to room temperature in vacuum (10^{-2} Pa), and the reference spectrum was recorded. After that, pyridine vapor was introduced to the

reduced catalyst until saturation adsorption. The desorption process was carried out by heat-treating the adsorbed sample at a heating rate of $5^\circ\text{C}/\text{min}$, and the IR spectra were recorded when the temperature reached 100°C , 150°C , 200°C , 300°C , and 350°C , respectively. Spectra were recorded at a resolution of 4 cm^{-1} and co-addition of 64 scans. The concentrations of Brønsted acid and Lewis acid sites were calculated according to the integrated absorbance of 1540 cm^{-1} and 1450 cm^{-1} , respectively [44].

The amount of carbonaceous deposit on the spent catalysts was determined using thermogravimetric analysis (TGA, TG 209F3, Netzsch) in flowing air of 50 mL/min at a heating rate of $10^\circ\text{C}/\text{min}$. Before the test, the spent 20Ni/HZSM-5(200) catalyst was washed by cyclopentane to remove the weakly adsorbed reactants and then dried at 80°C for 12 h.

3. Results and discussion

3.1. Activity evaluation of different catalysts

Firstly, a series of HZSM-5 supported Ni catalysts with different Ni loading were prepared by simple impregnation method for the HDO of PC. The $\text{SiO}_2/\text{Al}_2\text{O}_3$ of HZSM-5 is fixed at 25. The HZSM-5 exhibits very low activity, giving only 4.8 % yield of phenols (Fig. 1A). In contrast, Ni/HZSM-5 shows high HDO activity. The detected carbon increased progressively when the Ni loading changes from 2.5 wt % to 20 wt %. The C-C cracking products including C_6 and C_9 cycloalkanes were dominant when the Ni loading was below 10 wt %. There are still some C_{15} oxygenates and C_{15} aromatics unconverted. As the Ni loading increased to 10 wt %, the yield of C_{15} dicycloalkane rapidly increased to 37.7 % and the total yield of cycloalkanes could reach to 87.5 %. The yield of C_{15} dicycloalkane and the total yield of cycloalkanes were further increased as the Ni loading further increased to 20 wt %. However, when the Ni loading was 30 wt %, the yields of C_{15} dicycloalkane and cycloalkanes were slightly decreased with 5.3 % yield of C_{15} oxygenates (Fig. 1A).

In addition to metallic sites, the effect of $\text{SiO}_2/\text{Al}_2\text{O}_3$ ratio of HZSM-5 support on HDO of PC was also investigated (Fig. 1B). The molar ratio of $\text{SiO}_2/\text{Al}_2\text{O}_3$ varied from 25 to 360 while the Ni loading was kept as 20 wt %. The yield of C_{15} dicycloalkane increased significantly while the C-C

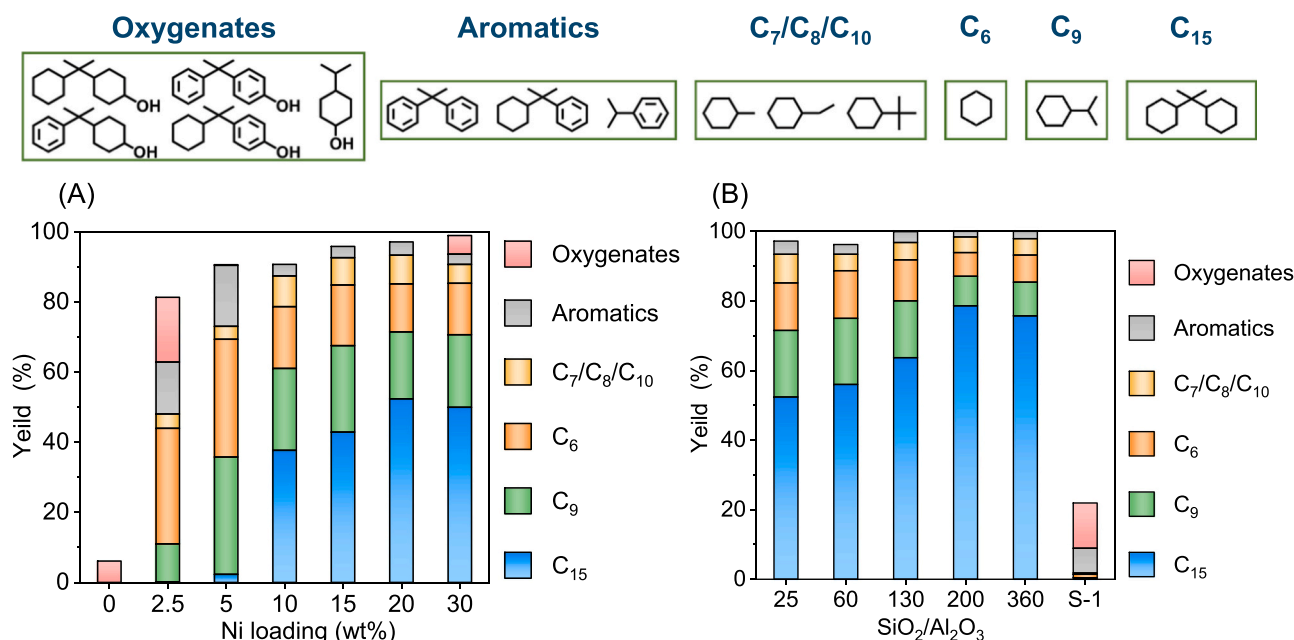


Fig. 1. HDO of PC over (x)Ni/HZSM-5(y) Catalysts. (A) Reaction profile of PC HDO as the function of the Ni loading of Ni/HZSM-5(25). (B) Reaction profile of PC HDO over as the function of the $\text{SiO}_2/\text{Al}_2\text{O}_3$ of 20Ni/HZSM-5. Reaction conditions: catalyst (0.1 g), PC pellets (0.3 g), cyclopentane (15 mL), initial H_2 (4 MPa), T (190°C), t (16 h).

cracking products (C_6 and C_9 cycloalkanes) decreased as the molar ratio of SiO_2/Al_2O_3 increased from 25 to 200. When the SiO_2/Al_2O_3 ratio was 200, the yield of C_{15} dicycloalkane reached to 78.4 %. However, a slightly decreased yield of C_{15} dicycloalkane was observed when the molar ratio of SiO_2/Al_2O_3 was 360. Furthermore, in the case of Ni/S-1 catalyst with the support without acidity, the detected carbon was 22.0 % with only 1.8 % yield of cycloalkanes (Fig. 1B). These results implied that the presence of dual catalytic functions is indispensable for the formation of aviation fuel range cycloalkanes from HDO of PC. The metal-acid balance (MAB) of Ni/HZSM-5 catalysts significantly affect the activity and product distribution, which will be discussed in latter section. As 20Ni/HZSM-5(200) catalyst achieved the best performance, it was chosen for all subsequent experiments.

3.2. Reaction pathways and mechanism for the HDO of PC

To understand the reaction pathways for HDO of PC, the time course of PC was investigated using the 20Ni/HZSM-5(200) catalyst (Fig. 2). At beginning of the reaction, the main products including C_{15} dicycloalkanes, C_{15} aromatics, C_{15} phenols and C_{15} cycloalcohols were detected. In addition, a small amount of C_6 – C_9 cycloalcohols and cycloalkanes were also observed, which due to the C-C cracking reaction. The yields of C_{15} aromatics and C_{15} oxygenates (C_{15} phenols and C_{15} cycloalcohols) increased simultaneously with the reaction time, reaching the maximum at 1 h, and then decreased. In the meantime, the yield of C_{15} dicycloalkanes sustained increased. This suggested that C_{15} aromatics and C_{15} oxygenates were the main intermediates for C_{15} dicycloalkanes. When the reaction time was 6 h, all these aromatics and oxygenates were completely converted to C_{15} dicycloalkanes via hydrogenation and HDO, respectively. The highest yield of total cycloalkanes reached to 99.3 % with 81.2 % of C_{15} dicycloalkane. In addition, the yields of C_6 and C_9 cycloalkanes were 7.9 % and 6.2 %, respectively. Further prolong the reaction to 16 h, the yield of C_{15} dicycloalkane and C-C cracking products (C_6 and C_9 cycloalkanes) kept almost the same. Compared with the previous work, the yield of cycloalkanes from HDO of PC is the highest (Table S1), demonstrating the significance of 20Ni/HZSM-5(200) catalyst.

During the conversion of PC, the formation of PC monomer, bisphenol A, were not observed while both C_{15} aromatics and C_{15} oxygenates (C_{15} monophenols and C_{15} cycloalcohols) with the similar yields were simultaneously formed. These implied that the depolymerization of PC probably proceeded by the direct hydrogenolysis of the C-O bond between benzene ring and ester group. To further confirm the C-O cleavage pathways, we investigated the catalytic performances of 20Ni/HZSM-5(200) on the HDO of the model compound, diphenyl carbonate, because of its similar chemical structure to PC (Fig. 3A). Scheme 1 shows three possible reaction routes for conversion of diphenyl carbonate: (1)

hydrogenation followed HDO, (2) hydrolysis followed HDO, (3) direct C-O hydrogenolysis followed by HDO and hydrogenation. In order to detect all the possible intermediate products during reaction, we controlled the reaction rate by lowering the reaction temperature. During the conversion of diphenyl carbonate, four different products including cyclohexane, benzene, phenol and cyclohexanol were detected. However, the ring saturation products of diphenyl carbonate were not observed, suggesting that the reaction pathway (1) can be excluded. To determine whether the first step of depolymerization of diphenyl carbonate is caused by hydrolysis, the time course of diphenyl carbonate was investigated using HZSM-5(200) catalysts (Table S2). Only a trace amount of phenol was detected and it was been maintained at a similar level even at longer reaction time. Thus, the hydrolysis pathway can also be excluded. Furthermore, the sum yields of cycloalkane and benzene are approximately equal to that of phenol and cyclohexanol in the HDO of diphenyl carbonate with 20Ni/HZSM-5(200), suggesting that the conversion of diphenyl carbonate proceeded through C-O bond cleavage rather than through hydrolysis. This further corroborates that the first step for the depolymerization of PC is direct C-O hydrogenolysis, forming aromatics and monophenols. The cycloalkanes were formed by the parallel hydrogenation of aromatics and HDO of monophenols. To identify the active site for the direct C-O hydrogenolysis during depolymerization of PC, the conversion of diphenyl carbonate over 20Ni/S-1 was conducted. It was shown that the reaction rate over 20Ni/S-1 was comparable to that over 20Ni/HZSM-5(200) (Table 1, entries 1 and 2), suggesting that the metal Ni site was responsible for the C-O cleavage during depolymerization of PC.

To further study the reaction pathway for the conversion of C_{15} monophenol over 20Ni/HZSM-5(200), HDO of phenol was carried out. At beginning of the reaction, besides cyclohexane, partially hydrogenated cyclohexanone and hydrogenated cyclohexanol were detected (Fig. 3B). However, benzene from direct C-O hydrogenolysis was not detected, suggesting that the C_{15} aromatics was not formed from the hydrogenolysis of C_{15} monophenol. In addition, the dehydration product, cyclohexene, was generated when HZSM-5 catalyzed cyclohexanol under N_2 atmosphere (Fig. 3E). Based on the above results, the reaction pathway for HDO of phenol to cyclohexane included: (1) hydrogenation of phenol to cyclohexanol via cyclohexanone as intermediate with metallic Ni sites; (2) dehydration of cyclohexanol into cyclohexene with acidic sites on HZSM-5; (3) finally hydrogenation of cyclohexene to cyclohexane with metallic Ni sites. This reaction pathway is the same as the previous reports on the HDO of lignin-derived phenols over bifunctional metal/zeolite catalysts [34,37,45].

The initial rates for each reaction step at the low conversions were determined based on the catalyst mass and exposed Ni sites (Table 1). The reaction rates were following the order of C-O bond hydrogenolysis of diphenyl carbonates < HDO of cyclohexanol \approx dehydration of

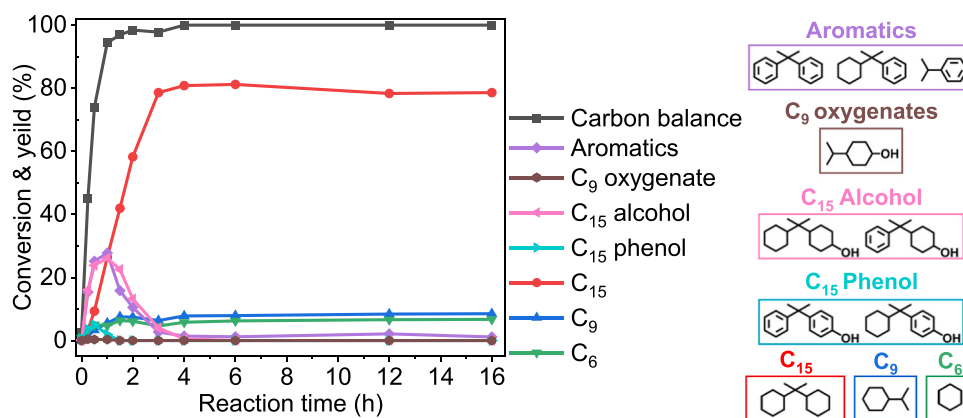


Fig. 2. Reaction profile of PC HDO over the 20Ni/HZSM-5(200) catalyst. Reaction conditions: catalyst (0.1 g), PC pellets (0.3 g), cyclopentane (15 mL), initial H_2 (4 MPa), T (190 °C).

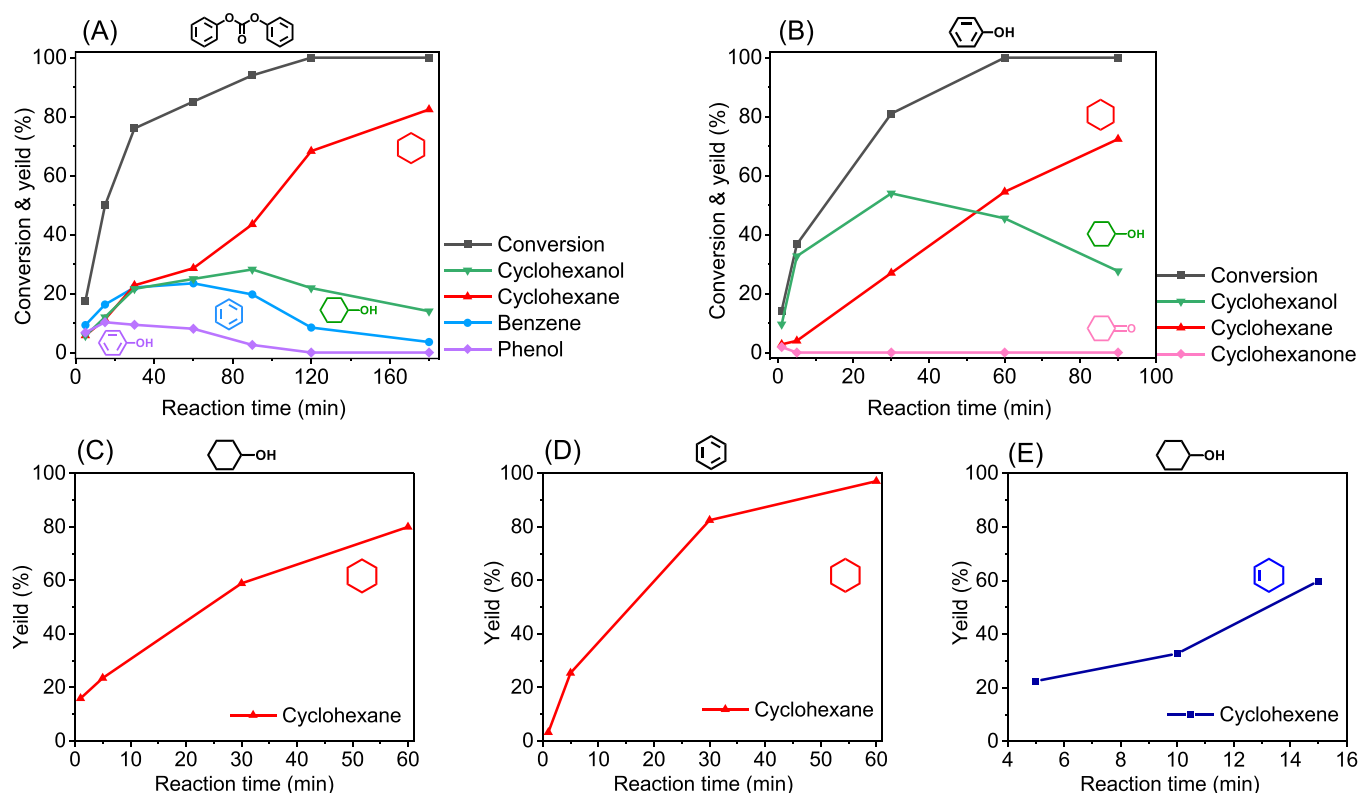
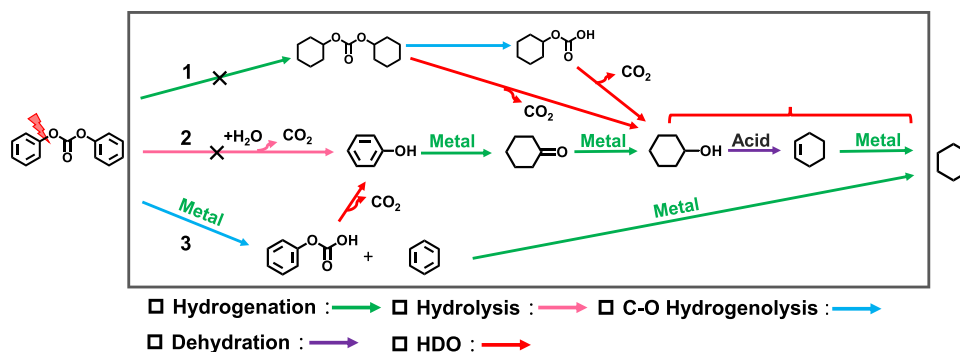


Fig. 3. Product distribution-reaction time curves for the catalytic conversion of: (A) Diphenyl carbonate, (B) Phenol, (C) Cyclohexanol, and (D) Benzene on 20Ni/HZSM-5(200). (E) The dehydration reaction of cyclohexanol catalyzed by HZSM-5(200). ^(A-D)Reaction conditions: catalyst (0.1 g), reactant (0.3 g), cyclopentane (15 mL), initial N₂ (0.5 MPa), H₂ (4 MPa), T (140 °C). ^(E)Reaction conditions: catalyst (0.1 g), reactant (0.3 g), cyclopentane (15 mL), initial N₂ (4 MPa), T (140 °C).



Scheme 1. Main reaction pathways of diphenyl carbonate HDO.

cyclohexanol < hydrogenation of benzene < hydroconversion of phenol. These results indicate that the C-O bond hydrogenolysis is the control step for the overall reaction with diphenyl carbonate. Given the similar reaction rate of HDO of cyclohexanol and dehydration of cyclohexanol, dehydration of cyclohexanol is the rate control step for the HDO of cyclohexanol. The benzene hydrogenation rate was faster than HDO of cyclohexanol, which is in accordance with the lower yields of C₁₅ aromatics during the PC conversion. It is worth noting that in the dual-functional catalytic system, the acid sites on the HZSM-5 can effectively promote the dehydration of cyclohexanol, thus driving the overall hydrodeoxygenation reaction.


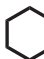

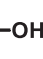

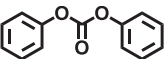
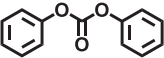
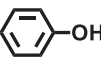
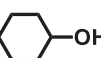

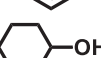
To understand the C-C cleavage pathways, the hydrogenolysis of bisphenol A (BPA) and saturated bisphenol A (4,4-(propane-2,2-diyl)dicyclohexanol) were exploited (Table S3). It was found that the C-C cracking products were detected in the case of hydrogenolysis of bisphenol A while no C-C cracking products were formed during the reaction of saturated bisphenol A. The main C-C cracking products were C₆

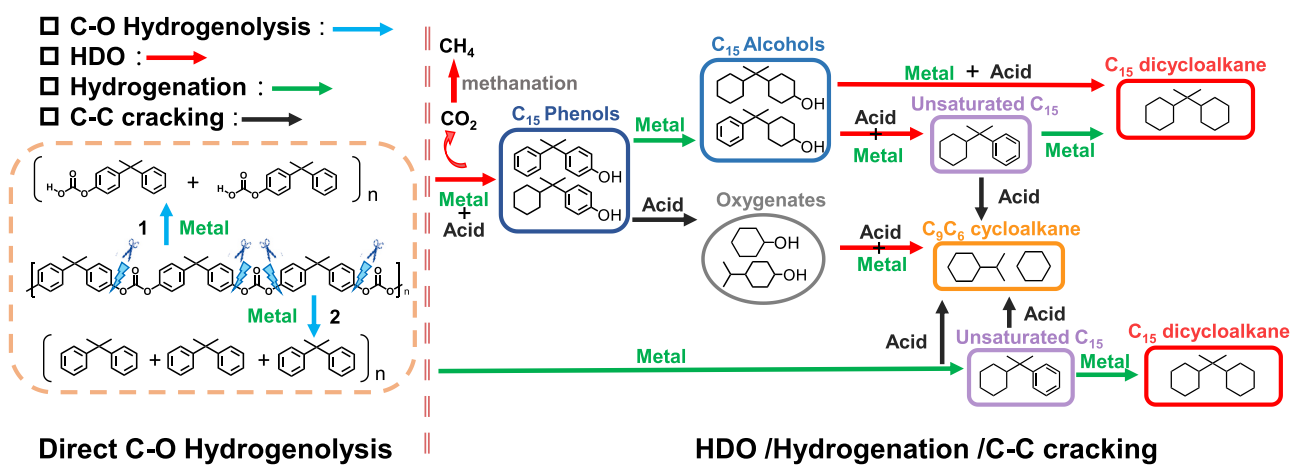
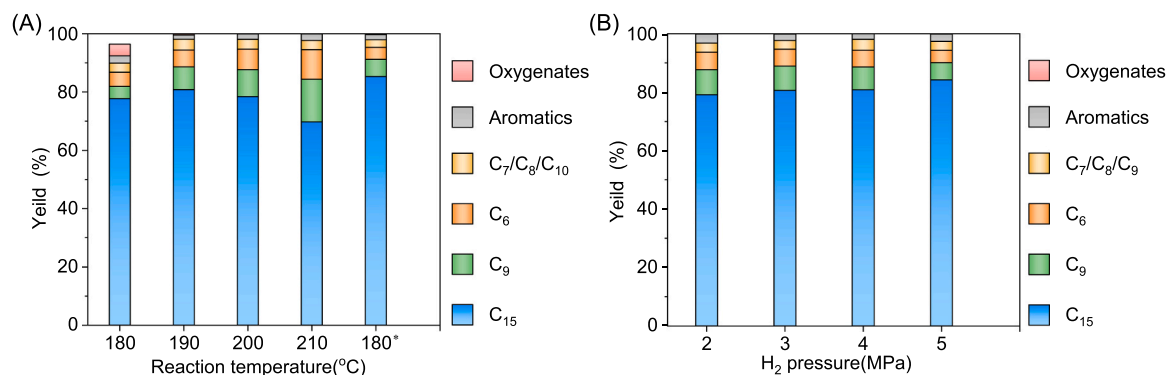
and C₉ cycloalkanes. Trace amount of C₉ cycloalcohol and C₉ aromatic were also observed. These results indicated that C-C bond cleavage is more likely to occur at the tertiary carbon center adjacent to the benzene ring. This can be further approved by the similar yields of C₁₅ dicycloalkane and C-C cracking products (C₆ and C₉ cycloalkanes) at longer reaction time (Fig. 2).

Based on above discussion, the overall reaction pathway for HDO of PC is depicted in Scheme 2. The conversion of PC into C₁₅ dicycloalkane mainly consisted of two stages: (1) firstly depolymerization of PC by the direct hydrogenolysis of C-O bonds adjacent to the benzene rings to form C₁₅ aromatics and C₁₅ monophenols randomly over metallic sites; (2) subsequently hydrogenation of C₁₅ aromatics rings over metallic Ni sites and HDO of C₁₅ monophenols over metal-acid dual sites on Ni/HZSM-5 to form C₁₅ dicycloalkane in parallel. The HDO of monophenols proceeded by the ring saturation by hydrogenation to form cycloalcohol over metallic Ni sites, following dehydration of cycloalcohol to cycloalkene over acidic sites on HZSM-5 and finally hydrogenation to

Table 1

The initial rates of various catalysts in different reactions.

Entry	Reactant	Catalyst	Conv. ^a (%)	Yield (%)					Reaction rate ^b (mmol·g ⁻¹ ·min ⁻¹)	Reaction rate ^c (mmol·mmol ⁻¹ ·min ⁻¹)
										
1		20Ni/S-1	24.6	8.5	2.9	4.5	8.7	0	0.69	19.3
2		20Ni/ HZSM-5 (200)	27.5	9.3	5.8	5.7	6.8	0	0.77	21.8
3		20Ni/ HZSM-5 (200)	36.7	0	4.0	32.7	\	0	2.40	67.7
4		20Ni/ HZSM-5 (200)	23.5	0	23.5	\	0	0	1.38	39.0
5		20Ni/ HZSM-5 (200)	25.4	\	25.4	0	0	0	1.92	54.1
6		HZSM-5 (200)	22.5	0	0	\	0	22.5	1.36	

Reaction conditions: catalyst (0.1 g), reactant (0.3 g), cyclopentane (15 mL), initial N₂ (0.5 MPa), H₂ (4 MPa), T (140 °C), t (5 min).^a The conversion was calculated as follows: conversion = (n_i-n_f)/n_i. The n_i and n_f stand for the moles of reactant in initial feed and final products;^b The reaction rate was calculated as follows: reaction rate = (mmol reactant consumed)/(g catalyst)/t;^c The reaction rate was calculated as follows: reaction rate = (mmol reactant consumed)/(mmol metal)/t.**Scheme 2.** Main reaction pathways of PC HDO.**Fig. 4.** (A) Effect of temperature on HDO of PC over 20Ni/HZSM-5(200) catalyst. Reaction conditions: catalyst (0.1 g), PC pellets (0.3 g), cyclopentane (15 mL), initial H₂ (4 MPa), t (4 h). 180 ° reaction conditions: catalyst (0.1 g), PC pellets (0.3 g), cyclopentane (15 mL), initial H₂ (4 MPa), t (16 h). (B) Effect of hydrogen pressure on HDO of PC over 20Ni/HZSM-5(200) catalyst. Reaction conditions: catalyst (0.1 g), PC pellets (0.3 g), cyclopentane (15 mL), T (190 °C), t (4 h).

cycloalkane on metallic Ni sites. The dehydration is the rate determining step in the HDO stage. The C-C cracking mainly occurred on the tertiary carbon adjacent to the benzene ring on acidic sites of HZSM-5 and thus C₆ and C₉ cycloalkanes were formed over Ni/HZSM-5. CO₂ and CH₄ was the main gaseous products in our system (Fig. S7). CO₂ was formed through the decarboxylation reaction of carbonate groups in PC, while CH₄ was generated by the methanation of CO₂ or the C-C bond cleavage of cyclic alkanes.

3.3. The effects of the reaction temperature and H₂ pressure

The effects of the reaction temperature and initial hydrogen pressure on the catalytic performance of the 20Ni/HZSM-5(200) were also investigated (Fig. 4). PC can react with full conversion in only 4 h when the temperature is higher than 190 °C. However, when the reaction temperature was 180 °C, a small amount (4 %) of oxygenates were still not converted. Further extending reaction time to 16 h, all the oxygenates were fully deoxygenated to cycloalkanes. The yields of cycloalkanes were almost the same at different reaction temperature. However, the yield of target C₁₅ dicycloalkane decreased with a concurrent increase in the yields of C₆ and C₉ cycloalkanes. This can be rationalized by high reaction temperature favoring C-C cracking reactions. The highest yield of C₁₅ dicycloalkane could reach to 85.3 % when the reaction temperature was 180 °C for 16 h.

Increasing H₂ pressure from 2 to 5 MPa exhibits no effect on PC conversion and the yield of cycloalkanes but an enhanced selectivity to C₁₅ dicycloalkane, suggesting less C-C cracking occurred at higher H₂ pressure. Because C-C cleavage mainly occurred at the tertiary carbon center adjacent to benzene ring, higher H₂ pressure favored hydrogenation of benzene ring and thus inhibited the C-C cracking.

3.4. Structure and physicochemical properties of fresh catalysts

To elucidate the relationship between the MAB of the catalysts and their performance, characterizations including XRD, SEM, TEM, H₂ pulse chemisorption, NH₃-TPD and Py-FT-IR were conducted.

XRD patterns of the reduced 20Ni/HZSM-5(y) samples are depicted in Fig. 5. All the samples showed the typical patterns of MFI structure, suggesting the loading of Ni didn't change the zeolites' structure. In addition, several diffraction peaks at $2\theta = 44.5^\circ$, 51.8° , and 76.4° , which are assigned to metallic Ni phase, were observed [41]. Calculated by Scherrer equation based on Ni(111) crystal plane ($2\theta = 44.5^\circ$), the average particle size of Ni on 20Ni/HZSM-5(25–360) catalysts are 43.1 nm, 45.4 nm, 42.9 nm, 44.4 nm and 40.6 nm respectively.

Fig. S1 and Fig. 6 shows the scanning electron microscopy (SEM) and transmission electron microscopy (TEM) images of Ni/HZSM-5 catalysts. SEM images showed that the HZSM-5 zeolites exhibited uniform coffin-shaped particles (216–615 nm) with relatively smooth surface. With Ni loading, the surfaces became rough (Fig. S1a–l), suggesting Ni

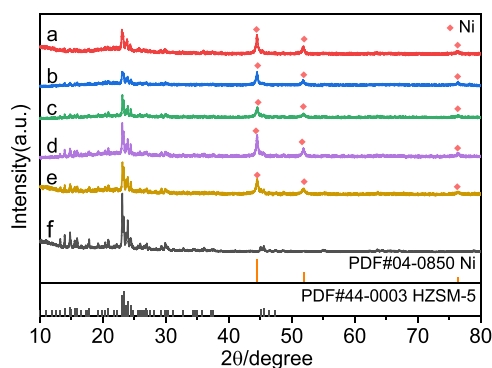


Fig. 5. XRD patterns of a 20Ni/HZSM-5(25), b 20Ni/HZSM-5(60), c 20Ni/HZSM-5(130), d 20Ni/HZSM-5(200), e 20Ni/HZSM-5(360) and f HZSM-5(200).

particles were successfully deposited on HZSM-5 surface. This can also be approved by the TEM characterization that the Ni particles surrounded the surface of HZSM-5 zeolites. The Ni particle size distributions of the samples were collected by statistical analysis of > 300 particles. All the samples showed similar average particle size of metal Ni (42.5 nm~47.0 nm), which is accordance with XRD analysis. In addition, BET surface area of 20Ni/HZSM-5(200) was lower than the pristine HZSM-5(200), which can be ascribed to the occupation of Ni particles on HZSM-5 (Table S4).

The quantity of accessible metal centers (n_{Ni}) of the Ni/HZSM-5 catalysts, measured by using H₂ pulse chemisorption, showed the samples with same Ni loading but different SiO₂/Al₂O₃ ratios have similar metal dispersions (Table 2).

The acid properties of 20Ni/HZSM-5(y) were determined by NH₃-TPD and Py-FT-IR (Fig. 7). The concentrations of Brønsted (c_B), Lewis (c_L) acid sites and total acid concentration are listed in Table 2. The acid density in 20Ni/HZSM-5(200) was reduced compared to pure HZSM-5(200) (Fig. S3a), which can be attributed to blockage of acid sites by loaded Ni particles on HZSM-5. NH₃ desorption temperature of the catalysts shifted to lower temperature as the SiO₂/Al₂O₃ ratio increased, suggesting the weakened acid strength. Moreover, the total acid concentration decreased as the SiO₂/Al₂O₃ ratio increased (from 1190.5 $\mu\text{mol}\cdot\text{g}^{-1}$ to 509.2 $\mu\text{mol}\cdot\text{g}^{-1}$). From Py-FT-IR, it can be seen that the Brønsted acid concentrations sharply decreased from 174.6 $\mu\text{mol}\cdot\text{g}^{-1}$ to 9.2 $\mu\text{mol}\cdot\text{g}^{-1}$ as the SiO₂/Al₂O₃ ratio increased from 25 to 360, which is in accordance with the results from NH₃-TPD. The presence of Brønsted acid sites on the catalyst is significantly essential for HDO reaction, which is important for generating alkanes [35,46].

3.5. The impact of metal-acid balance (MAB) on HDO activity and product distribution

As discussed above, the cooperation between the metallic sites and the acidic centers on HZSM-5 is of significance for the conversion of PC into cycloalkanes. In this regard, the metal-acid balance (MAB), which refer to the surface metal sites to Brønsted acid sites ratio, could determine the HDO activity and product distribution during PC conversion. Only the concentration of Brønsted acid sites was used for MAB calculations, since they are primarily responsible for dehydration activity of alcohols and the generation of the carbocation reaction intermediates [46–50].

To investigate the effect of MAB (n_{Ni}/n_A) on conversion of PC over Ni/HZSM-5 catalysts, the MAB was modulated by varying SiO₂/Al₂O₃ ratios of HZSM-5 zeolites. The MAB varied from 2.1 to 37.5 (Table 2). Based on the characterizations, all the Ni/HZSM-5 catalysts with same Ni loading exhibited similar average Ni particle sizes and dispersions (Table 2), which can decouple the effect of metal properties on the HDO of PC. Due to the different selectivity to the target C₁₅ dicycloalkane over different Ni/HZSM-5 catalysts, we define the formation rate of cycloalkanes (C₁₅ dicycloalkane, C₉ cycloalkane and C₆ cycloalkane) as HDO rate for the catalyst. It was found that the HDO rate increased upon the metal-to acid sites molar ratios (Fig. 8A), suggesting the acid sites were play the dominant role in the HDO activity. The dehydration of cyclohexanol with different HZSM-5 showed that the dehydration rate was strongly dependent with the acidic amount of HZSM-5, which is accordance with the HDO activities of various Ni/HZSM-5 zeolites. Since the dehydration of cycloalcohol is the control step during the HDO stage, we deduce that the acid sites mainly promote the dehydration rates and thus enhance the HDO activity. The product distribution over HZSM-5 with different MAB were also compared (Fig. 8B). The selectivity of target C₁₅ dicycloalkane decreased while the selectivity of C₆ and C₉ cycloalkanes increased as MAB decreased. This indicated that the higher number of the Brønsted acid site, favored the C-C cracking reaction [48–50]. According to the reaction mechanism, C-C cracking reaction mainly occurred at the tertiary carbon adjacent to benzene ring. In this regard, benzene ring saturation and C-C cracking are in a competitive manner.

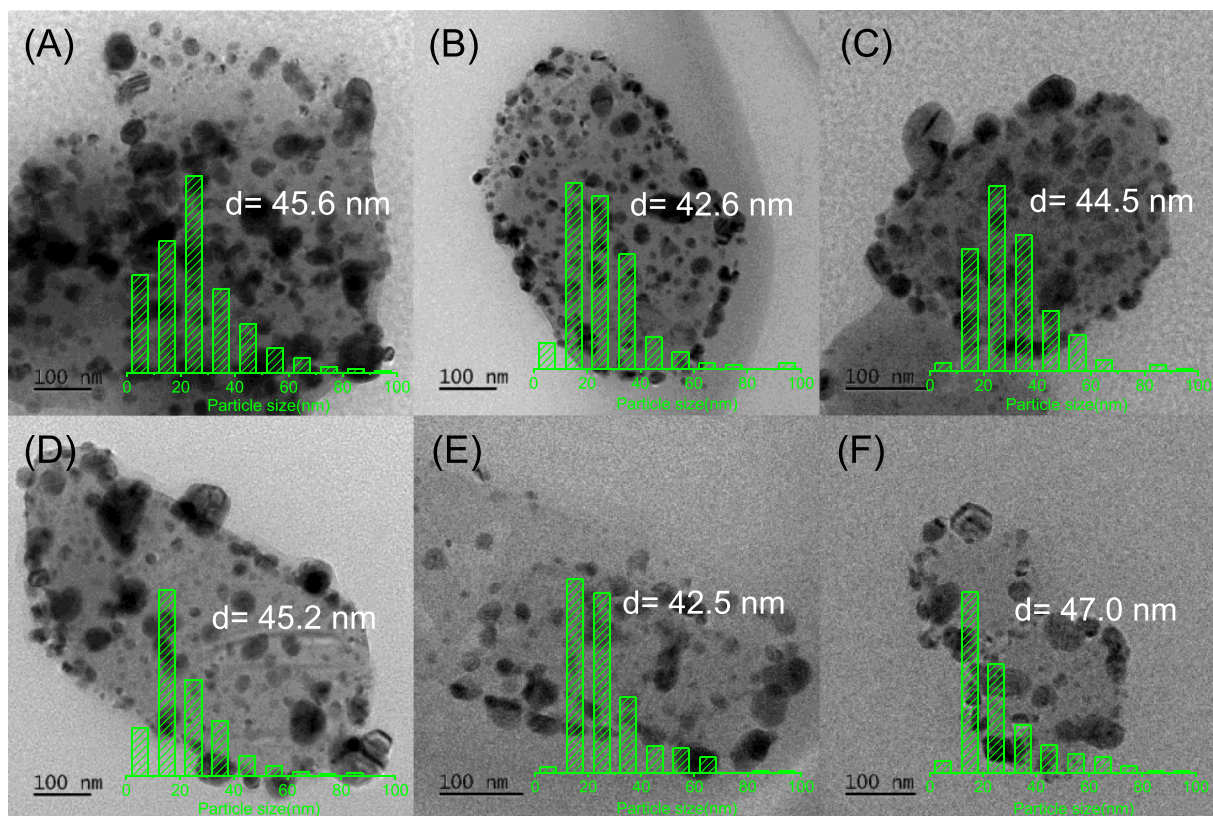


Fig. 6. TEM images of the (A) 20Ni/HZSM-5(25), (B) 20Ni/HZSM-5(60), (C) 20Ni/HZSM-5(130), (D) 20Ni/HZSM-5(200), (E) 20Ni/HZSM-5(360), (F) 20Ni/S-1.

Table 2

Characteristics of Ni/HZSM-5 catalysts.

Samples	d_{Ni}^a (nm)	D_{Ni}^b (%)	n_{Ni}^c ($\mu\text{mol/g}$)	Total Acidity ^d ($\mu\text{mol/g}$)	Acidity ^e ($\mu\text{mol/g}$)		MAB ^f (n_{Ni}/n_A)
					Brønsted	Lewis	
20Ni/HZSM-5(25)	45.6	0.56	362.7	1190.5	174.6	91.4	2.1
20Ni/HZSM-5(60)	42.6	0.59	359.5	1058.6	101.2	36.0	3.6
20Ni/HZSM-5(130)	44.5	0.59	363.7	778.5	28.6	15.0	12.7
20Ni/HZSM-5(200)	45.2	0.58	354.8	553.5	18.1	42.6	19.6
20Ni/HZSM-5(360)	42.5	0.59	342.6	509.2	9.2	25.9	37.5
20Ni/S-1	47.0	0.55	335.5	/	/	/	/

^a The average Ni particle size was determined by TEM.

^b The Ni dispersions was determined by H₂ pulse chemisorption.

^c The mole of surface nickel atoms (n_{Ni}) was calculated by H₂ pulse chemisorption.

^d Total acid concentration was measured by NH₃-TPD.

^e Brønsted acid concentrations and Lewis acid concentrations were measured by Py-FT-IR spectra.

^f The MAB refers to the surface Ni sites to Brønsted acid sites ratio.

The catalyst with lower MAB possessed insufficient metallic sites and exhibited lower activity for the hydrogenation of benzene ring than acid catalyzed C-C cracking reaction, resulting in reduced C₁₅ dicycloalkane formation. Consequently, there is a trade-off effect between HDO activity and the formation of C₁₅ dicycloalkane over Ni/HZSM-5 catalyst with different MAB. Among the catalysts, 20Ni/HZSM-5(200) possessed the appropriate MAB, thus showing good HDO activity and excellent selectivity to C₁₅ dicycloalkane.

3.6. The applicability of Ni/HZSM-5 catalyst for HDO of real PC wastes

The HDO of several representative PC plastics wastes including DVD disk, CD disk and PC sheet were carried out to investigate the applicability of Ni/HZSM-5 catalyst (Fig. 9). Under the same optimized reaction condition (190 °C, 6 h), the 20Ni/HZSM-5(200) catalyst can effectively catalyze HDO of DVD disk and CD disk into cycloalkanes with the total

yields of 98.1 % and 98.6 %. Moreover, the yield of C₁₅ bicycloalkane could reach to 81.8 % and 79.6 %, respectively, which were similar to that from virgin PC pellets. However, only 24.9 % yield of cycloalkanes can be obtained when PC sheet was used as the substrate, probably due to its higher recalcitrance and compactness. In order to convert PC sheet completely, the reaction temperature, PC sheet dosage and reaction time was optimized. It is expected that 99 % yield of cycloalkanes with C₁₅ bicycloalkane yield of 83.9 % can be achieved at 200 °C for 20 h by converting smaller amount of PC sheet (0.1 g). These results indicated that the applicability of Ni/HZSM-5 catalyst for HDO of various PC plastic wastes into cycloalkanes for sustainable aviation fuels, providing a new route to circular economy.

3.7. Stability of catalysts

Catalyst stability is a key parameter for potential use of a catalytic

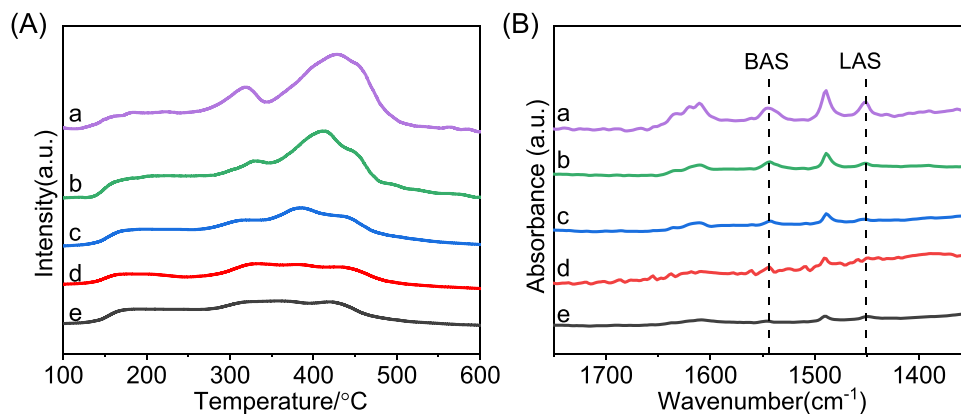


Fig. 7. (A). NH_3 -TPD profiles of 20Ni/HZSM-5(y) with the $\text{SiO}_2/\text{Al}_2\text{O}_3$ molar ratios of a 25, b 60, c 130, d 200, e 360. (B) Py-FT-IR spectra of 20Ni/HZSM-5(y) with the $\text{SiO}_2/\text{Al}_2\text{O}_3$ molar ratios of a 25, b 60, c 130, d 200, e 360 (spectra collected at 200 °C).

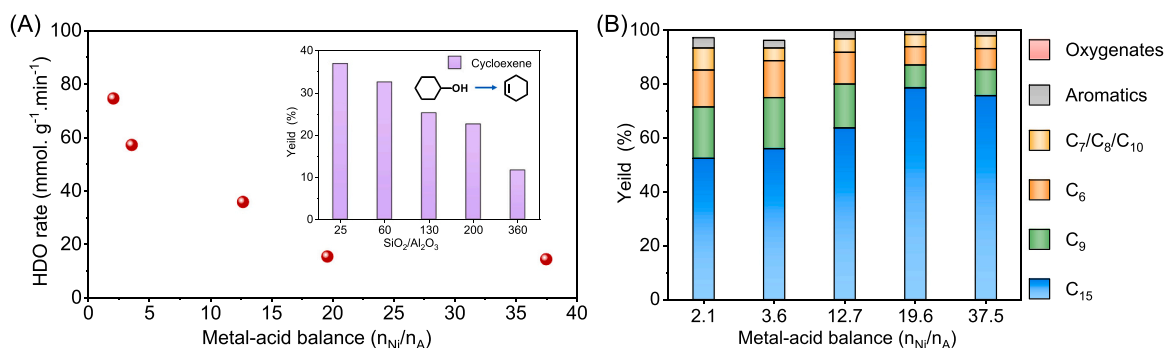


Fig. 8. HDO activity and product distribution as a function of the metal-acid balance ($n_{\text{Ni}}/n_{\text{A}}$).

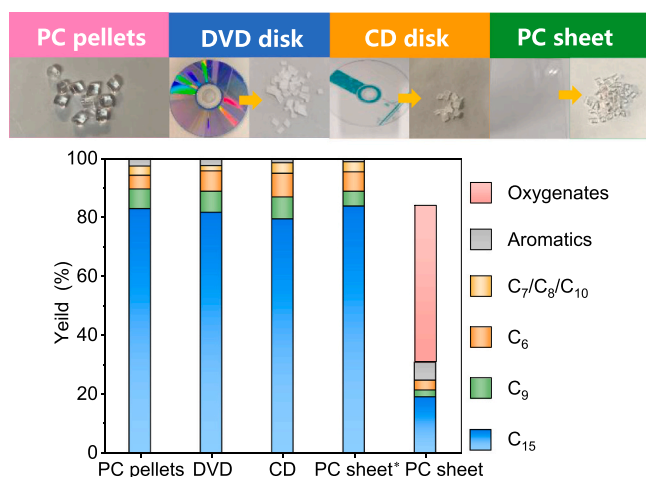


Fig. 9. HDO of real PC wastes over the 20Ni/HZSM-5(200) catalyst. Reaction conditions: catalyst (0.1 g), reactant (0.3 g), cyclopentane (15 mL), initial H_2 (4 MPa), T (190 °C), t (6 h). *Reaction conditions: catalyst (0.1 g), PC sheet (0.1 g), cyclopentane (15 mL), initial H_2 (4 MPa), T (200 °C), t (20 h).

process. To test for catalyst stability, the spent 20Ni/HZSM-5(200) catalyst was used dried in vacuum and directly used for the next run at 190 °C and 4 MPa H_2 for 6 h (Fig. 10A). The yield of cycloalkanes and C_{15} bicycloalkane decreased slightly ($\sim 2\%$) in the second run. Unfortunately, only about 9.5 % yield of cycloalkanes with C_{15} dicycloalkane yield of 3.3 % can be obtained in the third run, indicating the catalyst deactivation. TG analysis showed that a significant amount of carbon deposited on the catalyst, which could be the reason for the catalyst

deactivation (Fig. S4). The oxidation of the catalyst during collecting catalyst step can not be excluded. Consequently, the catalyst regeneration by calcination and reduction was performed to recover the catalyst activity. It was found that no notable changes in activity or selectivity were observed over six consecutive cycles. The yield of C_{15} dicycloalkane slightly decreased ($\sim 6\%$) while the yields of C-C cracking products (C_6 and C_9 cycloalkanes) and aromatics increased accordingly, which suggesting the slightly deactivation in hydrogenation of 20Ni/HZSM-5(200). To elucidate the small deactivation in hydrogenation, ICP-OES, XRD, and TEM characterizations for both the fresh and recovered catalysts. ICP-OES analysis of the reaction solution, after filtering off the catalyst, shows a slight leaching of Ni (0.0477 wt %, based on the total Ni amount). The XRD patterns of 20Ni/HZSM-5(200) after the sixth cycle showed that the peaks assigned to Ni metal became sharper (Fig. 10B), suggesting the sintering of the catalyst. The TEM images (Fig. 10C) showed that the average Ni particle size after the sixth cycle is 53.6 nm, which was larger than that of the fresh catalyst (45.2 nm), possibly due to sintering during regeneration process and reaction. Therefore, 6 % yield loss of C_{15} dicycloalkane in the sixth cycle could be ascribed to the co-effect of small amounts of metal leaching, and sintering of Ni particles in the catalyst.

4. Conclusions

We present a novel bifunctional Ni/HZSM-5 catalyst for conversion of PC plastics wastes into cycloalkanes for sustainable aviation fuels in high yield (99.3 %) with 81.2 % yield of C_{15} dicycloalkane under mild reaction conditions (190 °C, 4 MPa H_2). The overall reaction pathway for the conversion of PC into C_{15} dicycloalkane mainly includes two stages: (1) first, depolymerization of PC by the direct hydrogenolysis of C-O bonds adjacent to the benzene rings, and the random formation of C_{15} aromatics and C_{15} monophenols at metal sites; (2) subsequent

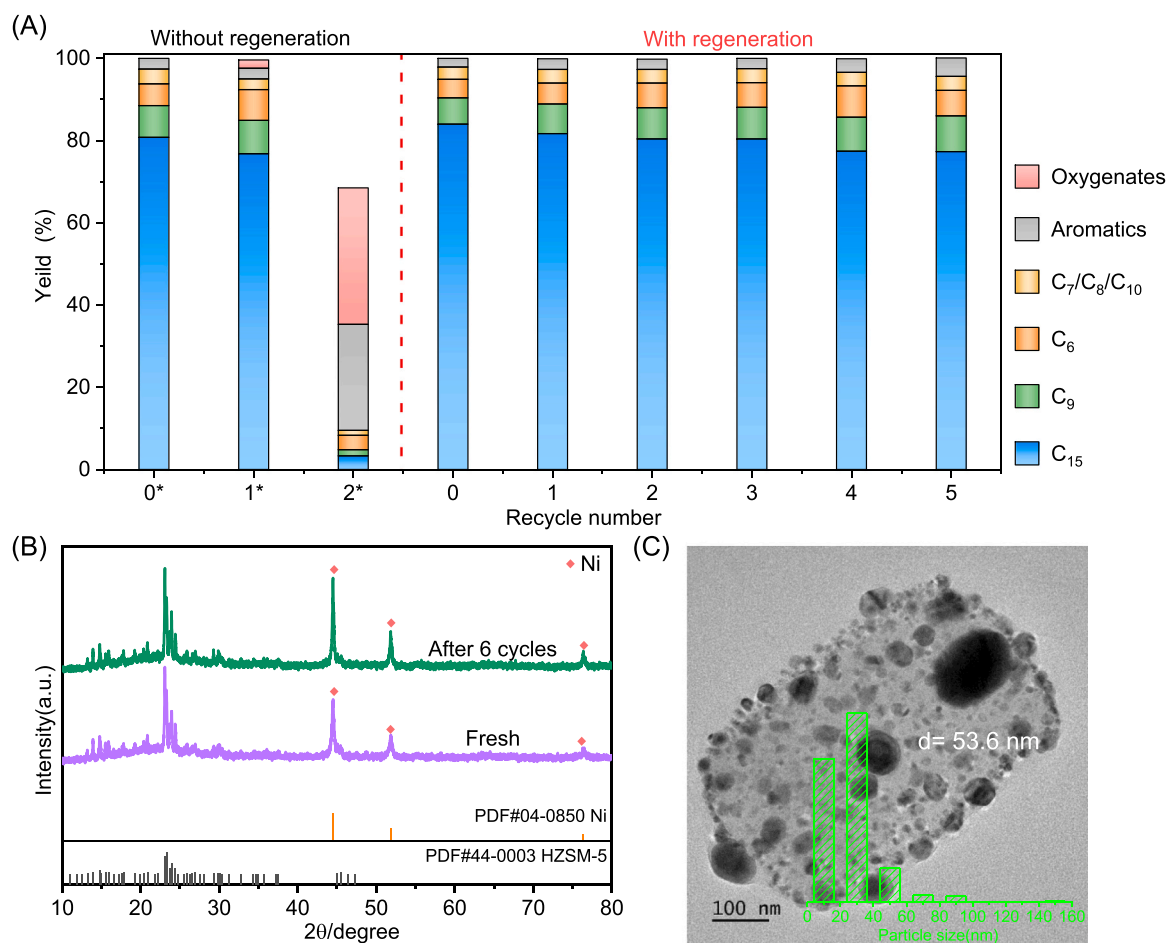


Fig. 10. (A) Recyclability of the 20Ni/HZSM-5(200) catalyst. Reaction conditions: catalyst (0.1 g), PC pellets (0.3 g), cyclopentane (15 mL), initial H₂ (4 MPa), T (190 °C), t (6 h). (B) XRD patterns of fresh catalysts after reduced and recovered catalyst after 6 cycles. (C) TEM image of recovered catalysts after 6 cycles.

parallel hydrogenation of C₁₅ aromatics rings on metal Ni sites and HDO of C₁₅ monophenols at metal-acid dual sites to generate C₁₅ dicycloalkane. The HDO of monophenols involved the ring saturation via hydrogenation at metal Ni sites, subsequent dehydration of cyclic alcohols to cycloalkenes at the acid sites of HZSM-5, and finally hydrogenation to cycloalkanes at metallic Ni sites. Dehydration is the rate-determining step at the HDO stage. The C-C cracking mainly occurred on the tertiary carbon adjacent to the benzene ring on acidic sites of HZSM-5, and then C₆~C₉ cycloalkanes were generated over Ni/HZSM-5. The synergy between metal sites and acid centers on Ni/HZSM-5 is critical to achieve this process. Besides, there is a trade-off effect between HDO activity and the selectivity of C₁₅ dicycloalkane over Ni/HZSM-5 catalyst with different MAB. Among the catalysts, 20Ni/HZSM-5(200) with suitable MAB showed good HDO activity and excellent selectivity to C₁₅ dicycloalkane. This catalyst can be reused at least 6 times without loss of activity. In addition, this catalyst is applicable to convert different PC plastic wastes (CD disk, DVD disk, PC sheet) into cycloalkanes with the yield up to 98 %. This process, that using non-precious Ni/HZSM-5 catalyst, can significantly reduce the cost of chemical upcycling of PC plastic wastes to valuable aviation fuel ranged cycloalkanes, making it more feasible for practical applications.

CRediT authorship contribution statement

Jieyi Liu: Investigation, Data curation, Writing – Original Draft. **Junde Wei:** Investigation & Validation. **Xiao Feng:** Investigation & Writing. **Mingxia Song:** Resources & Writing. **Song Shi:** Resource & Supervision. **Sibao Liu:** Conceptualization, Resources, Supervision,

Writing - review & editing, Funding acquisition. **Guozhu Liu:** Conceptualization, Resources, Supervision, Writing - review & editing.

Declaration of Competing Interest

The authors declare that they have no known competing financial interests or personal relationships that could have appeared to influence the work reported in this paper.

Data Availability

Data will be made available on request.

Acknowledgments

We thank the National Natural Science Foundation of China (22208243, 52276209, 22072147) for financial support.

Appendix A. Supporting information

Supplementary data associated with this article can be found in the online version at [doi:10.1016/j.apcatb.2023.123050](https://doi.org/10.1016/j.apcatb.2023.123050).

References

- [1] M. MacLeod, H.P.H. Arp, M.B. Tekman, A. Jahnke, The global threat from plastic pollution, *Science* 373 (2021) 61–65.
- [2] R.G. Santos, G.E. Machovsky-Capuska, R. Andrade, Plastic ingestion as an evolutionary trap: toward a holistic understanding, *Science* 373 (2021) 56–60.

- [3] C. Jehanno, J.W. Alty, M. Roosen, S. De Meester, A.P. Dove, E.Y.X. Chen, F. A. Leibfarth, H. Sardon, Critical advances and future opportunities in upcycling commodity polymers, *Nature* 603 (2022) 803–814.
- [4] F. Zhang, F. Wang, X. Wei, Y. Yang, S. Xu, D. Deng, Y.-Z. Wang, From trash to treasure: chemical recycling and upcycling of commodity plastic waste to fuels, high-valued chemicals and advanced materials, *J. Energy Chem.* 69 (2022) 369–388.
- [5] L.D. Ellis, N.A. Rorrer, K.P. Sullivan, M. Otto, J.E. McGeehan, Y. Román-Leshkov, N. Wierckx, G.T. Beckham, Chemical and biological catalysis for plastics recycling and upcycling, *Nat. Catal.* 4 (2021) 539–556.
- [6] C.-H. Wu, L.-Y. Chen, R.-J. Jeng, S.A. Dai, 100% atom-economy efficiency of recycling polycarbonate into versatile intermediates, *ACS Sustain. Chem. Eng.* 6 (2018) 8964–8975.
- [7] T. Do, E.R. Baral, J.G. Kim, Chemical recycling of poly(bisphenol A carbonate): 1,5,7-Triazabicyclo[4.4.0]dec-5-ene catalyzed alcoholysis for highly efficient bisphenol A and organic carbonate recovery, *Polymer* 143 (2018) 106–114.
- [8] J. Wei, J. Liu, W. Zeng, Z. Dong, J. Song, S. Liu, G. Liu, Catalytic hydroconversion processes for upcycling plastic waste to fuels and chemicals, *Catal. Sci. Technol.* 13 (2023) 1258–1280.
- [9] A.C. Fernandes, Reductive depolymerization as an efficient methodology for the conversion of plastic waste into value-added compounds, *Green. Chem.* 23 (2021) 7330–7360.
- [10] M. Chu, Y. Liu, X. Lou, Q. Zhang, J. Chen, Rational design of chemical catalysis for plastic recycling, *ACS Catal.* 12 (2022) 4659–4679.
- [11] H. Li, H.A. Aguirre-Villegas, R.D. Allen, X. Bai, C.H. Benson, G.T. Beckham, S. L. Bradshaw, J.L. Brown, R.C. Brown, V.S. Cecon, J.B. Curley, G.W. Curtzwiler, S. Dong, S. Gaddameedi, J.E. García, I. Hermans, M.S. Kim, J. Ma, L.O. Mark, M. Mavrikakis, O.O. Olafasakin, T.A. Osswald, K.G. Papanikolaou, H. Radhakrishnan, M.A. Sanchez Castillo, K.L. Sánchez-Rivera, K.N. Tumu, R. C. Van Lehn, K.L. Vorst, M.M. Wright, J. Wu, V.M. Zavala, P. Zhou, G.W. Huber, Expanding plastics recycling technologies: chemical aspects, technology status and challenges, *Green. Chem.* 24 (2022) 8899–9002.
- [12] E.V. Antonakou, K.G. Kalogiannis, S.D. Stefanidis, S.A. Karakoulia, K. S. Triantafyllidis, A.A. Lappas, D.S. Achillas, Catalytic and thermal pyrolysis of polycarbonate in a fixed-bed reactor: The effect of catalysts on products yields and composition, *Polym. Degrad. Stab.* 110 (2014) 482–491.
- [13] X. Song, F. Liu, L. Li, X. Yang, S. Yu, X. Ge, Hydrolysis of polycarbonate catalyzed by ionic liquid [Bmim][Ac], *J. Hazard. Mater.* 244–245 (2013) 204–208.
- [14] F. Liu, Z. Li, S. Yu, X. Cui, X. Ge, Environmentally benign methanolysis of polycarbonate to recover bisphenol A and dimethyl carbonate in ionic liquids, *J. Hazard. Mater.* 174 (2010) 872–875.
- [15] Y.-Y. Liu, G.-H. Qin, X.-Y. Song, J.-W. Ding, F.-S. Liu, S.-T. Yu, X.-P. Ge, Mesoporous alumina modified calcium catalyst for alcoholysis of polycarbonate, *J. Taiwan Inst. Chem. Eng.* 86 (2018) 222–229.
- [16] C.-H. Lin, H.-Y. Lin, W.-Z. Liao, S.-A. Dai, Novel chemical recycling of polycarbonate (PC) waste into bis-hydroxyalkyl ethers of bisphenol A for use as PU raw materials, *Green. Chem.* 9 (2007) 38–43.
- [17] E. Quaranta, C.C. Minischetti, G. Tartaro, Chemical recycling of poly(bisphenol A carbonate) by glycolysis under 1,8-diazabicyclo[5.4.0]undec-7-ene catalysis, *ACS Omega* 3 (2018) 7261–7268.
- [18] J. Payne, M.D. Jones, The chemical recycling of polyesters for a circular plastics economy: challenges and emerging opportunities, *ChemSusChem* 14 (2021) 4041–4070.
- [19] S.C. Kosloski-Oh, Z.A. Wood, Y. Manjarrez, J.P. de los Rios, M.E. Fieser, Catalytic methods for chemical recycling or upcycling of commercial polymers, *Mater. Horiz.* 8 (2021) 1084–1129.
- [20] S.S. Borkar, R. Helmer, F. Mahnaz, W. Majzoub, W. Mahmoud, M. Al-Rawashdeh, M. Shetty, Enabling resource circularity through thermo-catalytic and solvent-based conversion of waste plastics, *Chem. Catal.* 2 (2022) 3320–3356.
- [21] X. Wang, T. Jia, L. Pan, Q. Liu, Y. Fang, J.-J. Zou, X. Zhang, Review on the relationship between liquid aerospace fuel composition and their physicochemical properties, *Trans. Tianjin Univ.* 27 (2021) 87–109.
- [22] J. Nie, T. Jia, L. Pan, X. Zhang, J.-J. Zou, Development of high-energy-density liquid aerospace fuel: a perspective, *Trans. Tianjin Univ.* 28 (2022) 1–5.
- [23] S. Karatzos, J.S. van Dyk, J.D. McMillan, J. Saddler, Drop-in biofuel production via conventional (lipid/fatty acid) and advanced (biomass) routes. Part I, *Biofuels Bioprod. Bioref.* 11 (2017) 344–362.
- [24] D.R. Vardon, B.J. Sherbacow, K. Guan, J.S. Heyne, Z. Abdullah, Realizing “net-zero-carbon” sustainable aviation fuel, *Joule* 6 (2022) 16–21.
- [25] K.S. Ng, D. Farooq, A. Yang, Global biorenewable development strategies for sustainable aviation fuel production, *Renew. Sustain. Energy Rev.* 150 (2021), 111502.
- [26] X. Zhang, L. Pan, L. Wang, J.-J. Zou, Review on synthesis and properties of high-energy-density liquid fuels: Hydrocarbons, nanofluids and energetic ionic liquids, *Chem. Eng. Sci.* 180 (2018) 95–125.
- [27] H. Tang, Y. Hu, G. Li, A. Wang, G. Xu, C. Yu, X. Wang, T. Zhang, N. Li, Synthesis of jet fuel range high-density polycycloalkanes with polycarbonate waste, *Green. Chem.* 21 (2019) 3789–3795.
- [28] L. Wang, G. Li, Y. Cong, A. Wang, X. Wang, T. Zhang, N. Li, Direct synthesis of a jet fuel range dicycloalkane by the aqueous phase hydrodeoxygenation of polycarbonate, *Green. Chem.* 23 (2021) 3693–3699.
- [29] L. Wang, F. Han, G. Li, M. Zheng, A. Wang, X. Wang, T. Zhang, Y. Cong, N. Li, Direct synthesis of a high-density aviation fuel using a polycarbonate, *Green. Chem.* 23 (2021) 912–919.
- [30] Y. Jing, Y. Wang, S. Furukawa, J. Xia, C. Sun, M.J. Hülsey, H. Wang, Y. Guo, X. Liu, N. Yan, Towards the circular economy: converting aromatic plastic waste back to arenes over a Ru/Nb2O5 catalyst, *Angew. Chem. Int. Ed.* 60 (2021) 5527–5535.
- [31] K. Lee, Y. Jing, Y. Wang, N. Yan, A unified view on catalytic conversion of biomass and waste plastics, *Nat. Rev. Chem.* 6 (2022) 635–652.
- [32] Y.S. Yun, C.E. Berdugo-Díaz, D.W. Flaherty, Advances in understanding the selective hydrogenolysis of biomass derivatives, *ACS Catal.* 11 (2021) 11193–11232.
- [33] W. Liu, W. You, W. Sun, W. Yang, A. Korde, Y. Gong, Y. Deng, Ambient-pressure and low-temperature upgrading of lignin bio-oil to hydrocarbons using a hydrogen buffer catalytic system, *Nat. Energy* 5 (2020) 759–767.
- [34] C. Zhao, J.A. Lercher, Upgrading pyrolysis oil over Ni/HZSM-5 by cascade reactions, *Angew. Chem. Int. Ed.* 51 (2012) 5935–5940.
- [35] Y. Shi, E. Xing, K. Wu, J. Wang, M. Yang, Y. Wu, Recent progress on upgrading of bio-oil to hydrocarbons over metal/zeolite bifunctional catalysts, *Catal. Sci. Technol.* 7 (2017) 2385–2415.
- [36] B. Saini, A.P. Tathod, J. Diwakar, S. Arumugam, N. Viswanadham, Nickel nanoparticles confined in ZSM-5 framework as an efficient catalyst for selective hydrodeoxygenation of lignin-derived monomers, *Biomass. Bioenergy* 157 (2022), 106350.
- [37] C. Zhao, S. Kasakov, J. He, J.A. Lercher, Comparison of kinetics, activity and stability of Ni/HZSM-5 and Ni/Al2O3-HZSM-5 for phenol hydrodeoxygenation, *J. Catal.* 296 (2012) 12–23.
- [38] S. Li, L. Guo, X. He, C. Qiao, Y. Tian, Synthesis of uniform Ni nanoparticles encapsulated in ZSM-5 for selective hydrodeoxygenation of phenolics, *Renew. Energy* 194 (2022) 89–99.
- [39] W. Li, H. Wang, X. Wu, L.E. Betancourt, C. Tu, M. Liao, X. Cui, F. Li, J. Zheng, R. Li, Ni/hierarchical ZSM-5 zeolites as promising systems for phenolic bio-oil upgrading: Guaiacol hydrodeoxygenation, *Fuel* 274 (2020), 117859.
- [40] H. Wang, S.-a Wang, L. Guo, C. Qiao, Y. Tian, Hierarchical ZSM-5 supported Ni catalysts for hydrodeoxygenation of phenolics: effect of reactant volumes and substituents, *Chem. Eng. J.* 455 (2023), 140647.
- [41] F. Peng, L. Wang, X. Zhang, Q. Wang, Self-Pillared ZSM-5-supported Ni nanoparticles as an efficient catalyst for upgrading oleic acid to aviation-fuel-range-alkanes, *Ind. Eng. Chem. Res.* (2019).
- [42] S. Li, N. Li, G. Li, L. Li, A. Wang, Y. Cong, X. Wang, G. Xu, T. Zhang, Protonated titanate nanotubes as a highly active catalyst for the synthesis of renewable diesel and jet fuel range alkanes, *Appl. Catal. B: Environ.* 170–171 (2015) 124–134.
- [43] S. Li, N. Li, G. Li, L. Li, A. Wang, Y. Cong, X. Wang, T. Zhang, Lignosulfonate-based acidic resin for the synthesis of renewable diesel and jet fuel range alkanes with 2-methylfuran and furfural, *Green. Chem.* 17 (2015) 3644–3652.
- [44] C.A. Emeis, Determination of integrated molar extinction coefficients for infrared absorption bands of pyridine adsorbed on solid acid catalysts, *J. Catal.* 141 (1993) 347–354.
- [45] P. He, Q. Yi, H. Geng, Y. Shao, M. Liu, Z. Wu, W. Luo, Y. Liu, V. Valtchev, Boosting the catalytic activity and stability of Ru metal clusters in hydrodeoxygenation of guaiacol through MWW zeolite pore constraints, *ACS Catal.* 12 (2022) 14717–14726.
- [46] W. Luo, W. Cao, P.C.A. Bruijninx, L. Lin, A. Wang, T. Zhang, Zeolite-supported metal catalysts for selective hydrodeoxygenation of biomass-derived platform molecules, *Green. Chem.* 21 (2019) 3744–3768.
- [47] F. Chen, M. Shetty, M. Wang, H. Shi, Y. Liu, D.M. Camaioni, O.Y. Gutiérrez, J. A. Lercher, Differences in mechanism and rate of zeolite-catalyzed cyclohexanol dehydration in apolar and aqueous phase, *ACS Catal.* 11 (2021) 2879–2888.
- [48] Z. Dong, W. Chen, K. Xu, Y. Liu, J. Wu, F. Zhang, Understanding the structure–activity relationships in catalytic conversion of polyolefin plastics by zeolite-based catalysts: a critical review, *ACS Catal.* 12 (2022) 14882–14901.
- [49] S. Liu, P.A. Kots, B.C. Vance, A. Danielson, D.G. Vlachos, Plastic waste to fuels by hydrocracking at mild conditions, *Sci. Adv.* 7 (2021) eabf8283.
- [50] J.E. Rorrer, A.M. Ebrahim, Y. Questell-Santiago, J. Zhu, C. Troyano-Valls, A. S. Asundi, A.E. Brenner, S.R. Bare, C.J. Tassone, G.T. Beckham, Y. Román-Leshkov, Role of bifunctional Ru/Acid catalysts in the selective hydrocracking of polyethylene and polypropylene waste to liquid hydrocarbons, *ACS Catal.* 12 (2022) 13969–13979.